Full Paper

Israel Journal of Chemistry

DOI: 10.1002/ijch.202000097

Fluorescent Probes for the Supramolecular Interactions responsible for Binding of Polycyclic Aromatic Hydrocarbons to Hyperbranched Polyelectrolytes in Aqueous Media

Michael H. Ihde,[a] Ashley M. Steelman,[a, b] and Marco Bonizzoni*[a, c]

Abstract: Cationic poly(amidoamine) (PAMAM) dendrimers are known as good supramolecular hosts for a variety of smaller water-soluble guests. We expanded their binding scope to the uptake of very hydrophobic guests such as polycyclic aromatic hydrocarbons (PAH) in neutral aqueous solution. We used anthracene and pyrene as representatives of this family of hydrocarbons, and as capable fluorescent emitters to probe mode and location of interaction for these hydrocarbons with polycationic amine-terminated PAMAM dendrimers. We used steady-state and time-resolved fluorescence emission spectroscopy, as well as fluorescence anisotropy measurements and selective quenching experiments, to establish the mode and location of these binding interactions, demonstrating that, although these probes may look relatively similar, their interaction with PAMAM dendrimers is nevertheless significantly different. The results presented here provide insight into the attractive forces at play in the uptake of featureless hydrophobic PAH guests by hydrophilic PAMAM dendrimer hosts, whose applications span practical challenges including chemical separations, analytical discrimination, solubility and bioavailability enhancement of hydrophobic compounds.

Keywords: Dendrimers · Fluorescent probes · Host-guest systems · Non-covalent interactions · Supramolecular chemistry

1. Introduction

Globular polyelectrolytes such as dendrimers and micelles are extensively studied as encapsulating agents for small organic molecules.[1] In particular, dendrimers are hyperbranched polymers containing a central core from which repeat units extend outwards to form a three-dimensional structure. The divergent synthesis of such macromolecular architectures was first introduced in the late 1970s by Vögtle et al.;[2] many different families of dendritic structures have been introduced since.[3] One such class of dendrimers, poly(amidoamine) (PAMAM) dendrimers, was first prepared in the early 1980s by Tomalia et al.[4] These polyamides consist of a variety of divalent cores, most common being the 1,2-diaminoethane (ethylenediamine, *en*) core, with amidoamine repeating units; terminal primary amines represent further growth and branching points for these structures, with each new branching point starting a new generation of the dendrimer. Scheme 1 shows the chemical structure of a generation 1 (G1) PAMAM dendrimer, displaying the likely protonation (ca. 50%) of the surface amine groups at neutral pH, as shown previously for these dendrimers.[5] They are water soluble, commercially available, and highly ordered cationic polyelectrolytes that have received attention due to their interesting features, such as their well-defined globular structure and high loading capacity.[6]

The multi-valent binding capacity associated with these polyelectrolytes has been exploited extensively in our group, as demonstrated by their effectiveness as supramolecular hosts for the detection of organophosphates and biological phosphates,[7] and of carbohydrates,[8] using optical spectroscopic techniques. Because of these very promising results, wanting to continue our investigations aimed at a deeper understanding for some of the processes involved in encapsulation of small molecules in these polymers,[9] we embarked in studies to further clarify their modes of interaction with small-molecule analytes, particularly in neat water and other aqueous media. Our studies so far have shown that electrostatic interactions provide most of the driving force for complex formation, with hydrogen bonding and interactions of the pendant arms with aromatic moieties (i.e. CH-π and cation-π interactions) in the guest molecule providing more subtle differentiation in the resulting affinity between these polymers

[a] *M. H. Ihde, A. M. Steelman, M. Bonizzoni*
Department of Chemistry and Biochemistry, The University of Alabama, P.O. Box 870336, Tuscaloosa, AL 35487, United States
E-mail: marco.bonizzoni@ua.edu
[b] *A. M. Steelman*
Department of Chemistry, University of Kentucky, Lexington, KY 40506, United States
[c] *M. Bonizzoni*
The Alabama Water Institute, P.O. Box 870206, Tuscaloosa, AL 35487, United States

Supporting information for this article is available on the WWW under https://doi.org/10.1002/ijch.202000097

Israel Journal of Chemistry

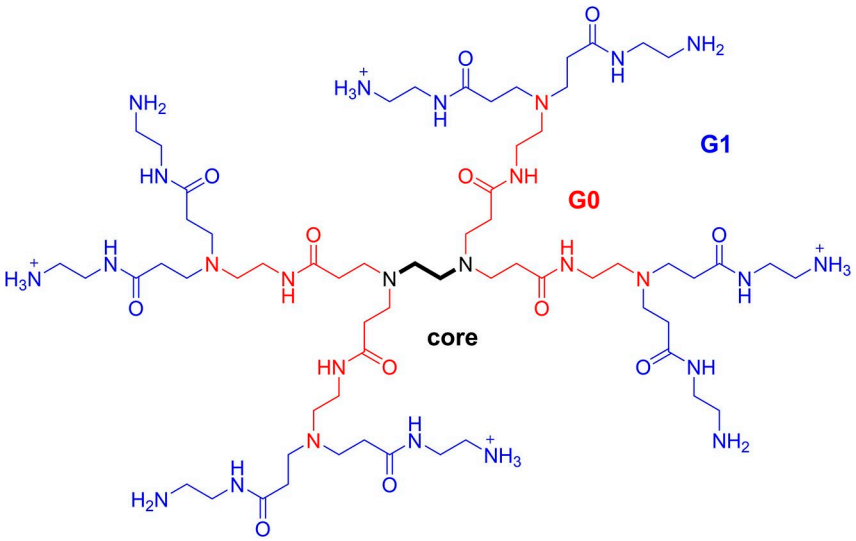

Scheme 1. Chemical structure of a first generation (G1) amine-terminated poly(amidoamine) (PAMAM) dendrimer in its most likely protonation state in water at neutral pH. Generations are highlighted in color: black = ethylenediamine core; red = generation 0 (G0); red + blue = generation 1 (G1).

and small water-soluble species. Here we concentrate on the effects of the unexpected and important interaction of the dendrimers with aromatic moieties in their guests. We present here insights into the use of amine-terminated PAMAM dendrimers as capable supramolecular hosts for simple, yet analytically relevant, polycyclic aromatic hydrocarbon (PAH) targets. The studies were conducted principally using fluorescence spectroscopic methods to probe the underlying interactions.

Polycyclic aromatic hydrocarbons (PAHs) provided a homogeneous family of hydrophobic aromatic compounds with pronounced and well-characterized fluorescence properties that could provide a valuable and varied family of probes to study the interaction of aromatic hydrophobics with these macromolecules. PAHs are also powerful pollutants with mutagenic and carcinogenic properties, whose determination through non-covalent sensing methods is important for environmental and health applications,[10] so characterizing their uptake into polymeric systems could also foster further applications towards their sensing and remediation. These compounds occur in many natural sources, however, emissions from pyrogenic sources such as fossil fuels and industrial manufacturing lead to their unwanted introduction into the environment.[11] Thus, research efforts attempt to address the detection of these compounds, despite their uncharged and non-polar nature, featureless chemical structure, and lack of functional groups.[12] In addition to chemical detection applications, understanding these interactions would also impact other problems, such as hydrophobic drug dissolution, modulation of drug bioavailability, and problems in separation science.

For this study, the fluorescence emission response of anthracene and pyrene (Scheme 2) was investigated upon their

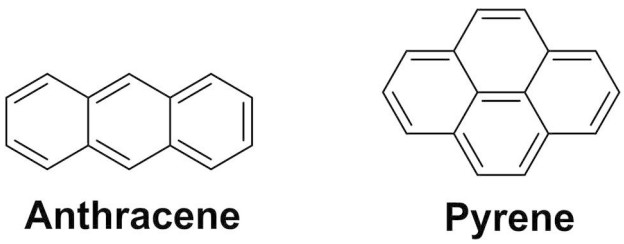

Scheme 2. Chemical structures of anthracene (left) and pyrene (right) as representative PAHs used as guest binding probes with amine-terminated PAMAM dendrimers.

interaction with amine-terminated PAMAM dendrimers. These PAHs were chosen as representative examples for their relatively simple chemical structure, their ready availability, and their intense, well-characterized fluorescence emission properties.[13] To evaluate the uptake of PAH guests by dendrimer host in neutral water despite the PAH's low solubility in this medium, a dissolution testing method was used, a technique often associated with the determination of solubility properties of pharmaceuticals.[14]

2. Results and Discussion

Thin-film dissolution experiments. For this method, stock solutions of PAH guests were prepared in hexanes; small aliquots (200–300 μL) of these solutions were added to multiple cuvettes and the solvent removed under a stream of nitrogen to deposit a constant amount of PAH in each cuvette. We made sure to deposit an amount of hydrocarbon much greater than what could be solubilized by water alone, and

large enough to ensure that only a fraction of the available PAH would be brought into solution by the polymer to ensure that the free dissolved hydrocarbon would always be maintained at a constant concentration by its natural dissolution equilibrium in the presence of the solid in the film. To the cuvettes were added buffered aqueous solutions containing increasing concentrations of three generations of PAMAM dendrimer (G3-G5). These polymer generations were chosen because they strike an optimal balance between large size and affordable cost, and therefore the findings would be more relevant for practical application. In fact, dendrimers smaller than G3 do not display high enough affinity to be viable in the desired applications.[15] On the other hand, larger dendrimers might perform better than those reported here, however they are exponentially more expensive than the smaller generations due to difficulty in obtaining them in high purity. All aqueous solutions were buffered to pH 7.4 using 50 mM 4-(2-hydroxyethyl)-1-piperazineethanesulfonic acid (HEPES); we were interested in neutral aqueous solutions because of the relevance of such conditions to both physiological and environmental applications.

Once prepared, the cuvettes were allowed to equilibrate overnight at room temperature, after which a fluorescence spectrum of the solution in each cuvette was taken, upon excitation at 350 nm. We obtained promising results with anthracene (Figure 1), with a linear increase in the fluorescence emission signal for anthracene as the concentration of amine-terminated PAMAM dendrimer was increased, indicating that more anthracene was being brought into solution as the dendrimer was added. This result, although encouraging, may have been influenced by the slight change in the composition of the solvent as larger quantities of the dendrimer stock solution was added (the dendrimer stock is made up in methanol), with a concomitant reduction in polarity of the solvent. Higher generations of PAMAM dendrimer caused proportionally greater amounts of anthracene to dissolve from the thin film into solution (see Figure 1, right), but a slightly larger amount of MeOH was added in with the larger dendrimers: therefore in these conditions we could not yet confirm that the observed effect was completely due to the polymer.

Also based on our previous experience with hydrophilic guests to these dendrimers,[9b] we propose that the most important supramolecular interactions responsible for anthracene binding are the cation-π interactions between the aromatic anthracene and the positively charged ammonium group at the dendrimer's surface, rather than the interactions between the non-polar hydrocarbon guests and the hydrophobic interior of the dendrimer. These interactions were responsible for hydrocarbon uptake from solution into a complex with the dendrimer, which in turn caused the dissolution of further anthracene from the thin film reservoir, as required by anthracene's natural solubility equilibrium in water. We also considered the change in ionic strength of the solution caused by the addition of the macromolecular polyelectrolyte as a possible cause for the increase in anthracene's emission. However, higher electrolyte concentrations are known to decrease the solubility of anthracene and other aromatics in water solutions;[16] this, of course, would *lower* the observed emission signal, and yet in our experiment we observed an *increase* in that signal.

We confirmed that an increase in ionic strength alone would not enhance anthracene's fluorescence by repeating the same experiment but using a polyanionic carboxylate-terminated PAMAM. Such carboxylate-terminated dendrimers are referred to as "half-generation" PAMAM (e.g. G4.5 is the carboxylate-terminated, negatively charged equivalent of the amine-terminated polycationic G5). The similarly sized polycarboxylate PAMAM G3.5 and polyammonium G4 dendrimers were both probed using anthracene as described above. Although they have opposite charges, the two dendrimers represent similar generations and are otherwise comparable in

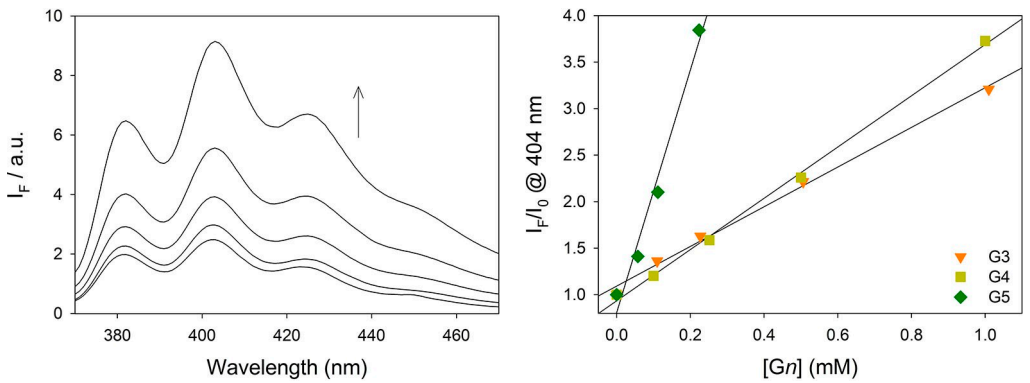

Figure 1. (Left): Representative fluorescence spectra of anthracene brought into solution from a thin film in buffered water (pH = 7.4 using HEPES) as a function of increasing concentration of G4 amine-terminated PAMAM dendrimer. (Right): Comparing fluorescence emission profiles for anthracene as a function of the total amount of G3-G5 PAMAM added; the black solid lines were obtained from linear regression analysis (λ_{exc} = 350 nm; total deposited anthracene = 1.12 μmol). The corresponding fluorescence emission spectra with G3 and G5 are shown in Figure S1 in the Supporting Information.

structure, size, and mass (64 surface groups; 14.2 kDa and 12.9 kDa for G4 and G3.5, respectively). The results, shown in Figure 2, indicate that the presence of G3.5 PAMAM dendrimer caused a *decrease* in anthracene emission, attributed to the increased ionic strength in solution, which caused the amount of free anthracene in solution to decrease by changing the properties of the bulk solvent.

On the other hand, in similar experiments conducted with pyrene instead of anthracene we observed very similar quenching behaviors when pyrene saturated solutions were exposed to either the cationic G4 and the anionic G3.5 (Figure S3), indicating that the peripheral functional groups on the dendrimer are less involved in the binding of pyrene to these dendrimers and, at the same time, that the hydrocarbon is bound in a position more accessible to the tertiary amine quenchers found in the inner layers of these dendrimers. This led us to conclude that the main driving force for the binding of pyrene to these dendrimers is likely to be hydrophobic interactions rather than charge-π interactions.

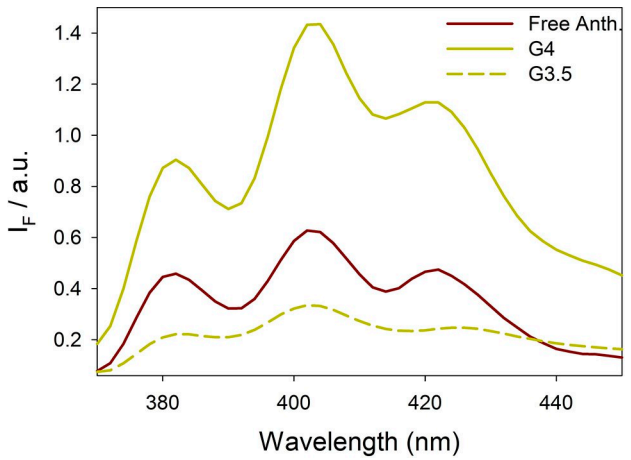

Figure 2. Thin film solubilization experiments of anthracene, comparing the effectiveness of positively (G4) and negatively (G3.5) charged poly(amidoamine) (PAMAM) dendrimers (anthracene = 16.9 μmol, λ_{exc} = 350 nm, [G*n*] = 0.10 mM). The emission spectrum from a saturated solution of free anthracene is included as a reference. All measurements were conducted in H_2O solution buffered to pH 7.4 in HEPES.

Pyrene was further used as a second fluorescent probe with unique and well-known emission characteristics. Specifically, pyrene is known to form excited-state dimers (excimers) when concentrations are high enough to permit an excited-state pyrene to come into close proximity with another ground-state molecule.[13a] However, the natural solubility of pyrene in neutral buffered water is too low for the free pyrene in solution to exhibit excimer emission under the experimental conditions outlined above. Therefore, observing emission from the excimer species in the presence of the PAMAM dendrimers (centered at $\lambda_{em.}$ = 470 nm) would be a direct indication that pyrene molecules have been forced into closer proximity through binding to the dendrimer; in other words, it would be direct evidence of binding of multiple molecules of pyrene to the dendrimer.

Thin-film dissolution experiments were conducted for pyrene according to the same procedure previously described for anthracene. As more cationic G3-G5 PAMAM dendrimer was added, a noticeable excimer band was formed in the fluorescence emission spectrum, upon excitation at 338 nm, which was otherwise not observed for free pyrene in water solution in the absence of PAMAM. Moreover, the intensity of this excimer band was linearly dependent on the PAMAM concentration, with a more pronounced dependence for higher generations of PAMAM. These results for pyrene are presented in Figure 3. The emergence of this excimer band strongly supported the hypothesis that the increase in fluorescence emission signal of PAH was due to supramolecular complex formation between the PAH and

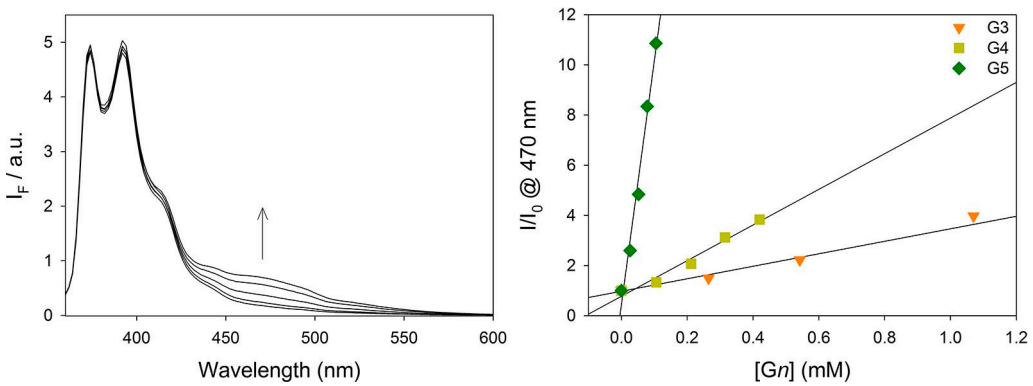

Figure 3. (Left): Fluorescence emission spectra of pyrene from thin film dissolution testing in buffered H_2O (pH = 7.4 using 50 mM HEPES) as a function of increasing concentration of G4 amine-terminated PAMAM dendrimer. The more structured emission bands at 374–394 nm correspond to the monomer form; the unstructured emission band centered at 470 nm corresponds to the excimer form. (Right): Profiles of the normalized fluorescence emission of pyrene's excimer as a function of increasing amounts of G3-G5 PAMAM (λ_{exc} = 338 nm; total deposited pyrene = 1.07 μmol). The corresponding fluorescence emission spectra using G3 and G5 are shown in Figure S2 in the Supporting Information.

dendrimer, leading to a net increase in PAH solubilization into water. In this context, pyrene is a particularly useful "dual-channel" probe: its monomer emission, around 390 nm, reports on the concentration of free pyrene in solution; as shown in Figure 3, this concentration is controlled by the probe's thermodynamic dissolution equilibrium so it does not change during the course of the experiment as long as solid pyrene is still present on the walls of the experimental vessel. On the other hand, the excimer emission at 470 nm reports on the amount of pyrene bound to the dendrimer, whose molecules are forced close enough to each other for excited state complexes to form; this emission signal increases markedly with the addition of the dendrimer hosts. Furthermore, the slope of the latter increasing trend is a measurement of the relative "loading capacity" of each generation of these polymers.

In the case of pyrene, we hypothesize that cation-π interactions are no longer the main driving force of the macromolecule-hydrocarbon interaction as they were with anthracene; instead, hydrophobic effects are more important to force pyrene inside the dendrimer. In fact, charge-π interactions in these systems are limited to the region of the dendrimer near the surface, exposed to the solvent, where the charged ammonium ions participating in these interactions are found.[17]

Strict control of bulk solution properties. We mentioned that, because PAMAM stock solutions are made up in MeOH and have different concentrations for each generation, increasing the concentration of PAMAM also resulted in an unwanted and concomitant increase in concentration of MeOH in the bulk solution, which may skew the reported results. To confirm that anthracene uptake was not a simple side-effect of a reduction in solution polarity caused by the MeOH, the same dissolution experiments were conducted at a constant concentration of G3-G5 dendrimer after adjusting the concentration of MeOH in each solution to the same value, thereby eliminating any bulk polarity effect. Results from these experiments are presented in Figure 4. For anthracene, an increase in the fluorescence emission signal was observed, which strongly suggests anthracene binding and uptake by the dendrimer. For pyrene, on the other hand, an opposite trend was observed; i.e. there is a noticeable reduction of pyrene's emission in the presence of the PAMAM dendrimer. Furthermore, the excimer emission signal was no longer visible in these conditions.

These preliminary results indicated that further investigation was needed to determine the modes of interaction of these cationic dendritic hosts with hydrophobic aromatics, including PAHs. We therefore turned to steady-state fluorescence anisotropy, time-resolved fluorescence spectroscopy, and selective quenching experiments to probe location and mode of binding.

Fluorescence Anisotropy Measurements. Fluorescence anisotropy experiments were conducted to confirm binding of the PAH probes to cationic PAMAM dendrimers. If bound to the larger polyelectrolytes, the PAH probe's anisotropy signal was expected to increase relative to that of the small-molecule fluorophore, free in solution. Free rotation of small molecules in solution occurs about 2 orders of magnitude faster than the intrinsic fluorescence lifetime of the PAH fluorescent probes used here. Thus, these small fluorophores will have isotropic polarization of their fluorescence emission, when free in solution and excited with plane polarized light (i.e. a low fluorescence anisotropy signal). However, the rotational diffusion rate of the complex formed by these probes upon binding to the much larger PAMAM macromolecule is dominated by the slower tumbling rate of the larger host, resulting in highly anisotropic polarization of the fluorescence emission of this complex, i.e. a high fluorescence anisotropy signal.

Thin-film dissolution experiments were carried out at a constant G3-G5 PAMAM concentration ([G*n*] = 0.1 mM).

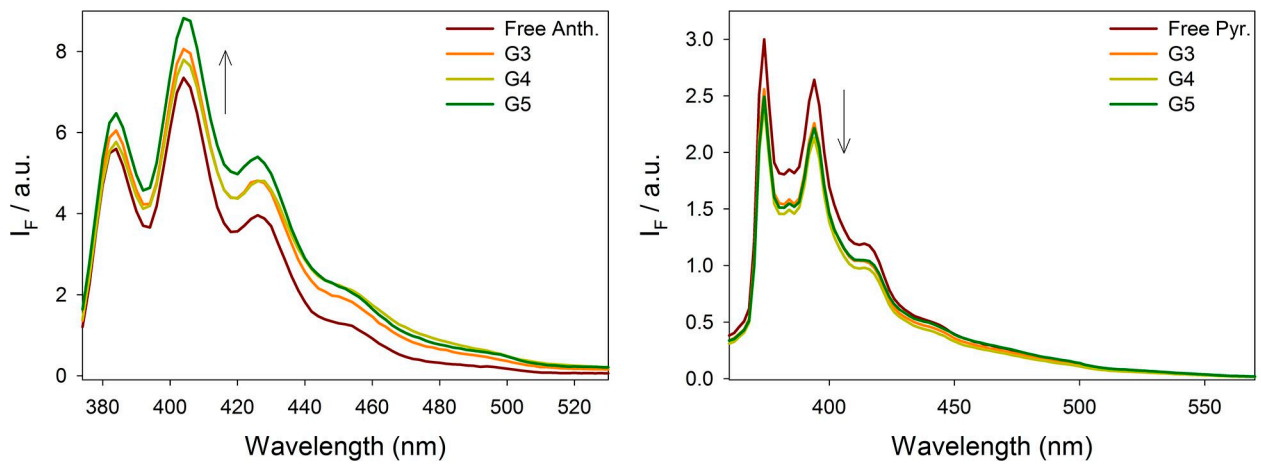

Figure 4. Fluorescence emission spectra of anthracene (left) and pyrene (right) solutions in equilibrium with a thin film of the respective solid, in H_2O solution buffered to pH 7.4 with 50 mM HEPES, in the presence of a constant concentration of dendrimer ([G*n*] = 0.1 mM) and 7.2% methanol (anthracene = 1.90 μmol, pyrene = 1.56 μmol, anthracene λ_{exc} = 350 nm; pyrene λ_{exc} = 338 nm).

Four 1 cm quartz cuvettes were prepared containing a thin film of each PAH probe, obtained by evaporation of a solution in hexanes as described previously; each cuvette was filled to a final volume of 3 mL with buffer and a calculated amount of G3-G5 dendrimer stock solution in methanol was added to each cuvette to achieve [dendrimer] = 0.1 mM. Once again, care was taken to ensure that each cuvette solution contained the same percent volume of methanol (7.2% MeOH) for all dendrimers. We also ensured that the dendrimer concentration was low enough to avoid interference from the PAMAM dendrimers' weak intrinsic emission,[18] which may interfere with anisotropy measurements (see Figure S4 and S5).

The solutions were then stored in the dark at room temperature overnight to reach equilibrium. Multiple anisotropy measurements were then taken for each cuvette, with the results presented in Figure 5. For both fluorescent hydrocarbon probes under study, there is a clear increase in fluorescence anisotropy going from free PAH to higher dendrimer generations (G3 to G5). The trend provided further evidence that the PAH probe is bound to the dendrimer. The observed increasing trend in anisotropy for the complexes of each PAH probe with the G3 vs. G4 vs. G5 PAMAM dendrimers agrees with expectation; the larger higher generation PAMAM dendrimers can accommodate more PAH guest molecules, increasing the fraction of the total PAH that is bound to the polymer, which in turn causes a corresponding increase in the fluorescence anisotropy signal.

The relatively low absolute values of the measured anisotropy signal for both PAH probes are likely due to the presence of free probe in solution, dissolved from the thin film deposited on the cuvette's walls according to its solubility equilibrium. In fact, the small unbound probe has a very low anisotropy signal. Since the solution's overall anisotropy is an average over all emitting forms of each probe, weighted by their molar fractions, the relatively high proportion of unbound probe in solution, with its low anisotropy signal, considerably depresses the ensemble average reading. It is also noteworthy that, counterintuitively, the anisotropy signal for the smaller anthracene probe is higher than the slightly larger pyrene's. This can either be due to tighter binding for anthracene than for pyrene, which increases the fraction of anthracene bound overall, thus increasing its relative contribution to the anisotropy signal; to the possibility of different degrees of internal mobility in each probe's complex, with the pyrene being more free to move even while bound; or, ultimately, to higher intrinsic anisotropy of anthracene vs. pyrene.[13a,19] Fortunately, the absolute value of the anisotropy is not important here; the trends are, and the information gleaned from those unequivocally supports tight binding of these hydrocarbon probes to the PAMAM cationic polyelectrolytes.

Time-resolved Fluorescence Measurements. Fluorescence lifetime determinations were carried out on the complexes of these hydrophobic PAH probes with the G3-G5 PAMAM dendrimers as well. Four cuvettes were prepared and equilibrated overnight with an equal concentration of PAMAM dendrimer for each generation ([G*n*] = 0.1 mM), as mentioned previously, and time-resolved fluorescence measurements were then conducted to determine the fluorescence emission lifetimes of the PAH probes upon binding. The exponential decay profiles for both PAHs with G3-G5 PAMAM dendrimers are displayed in Figure 6. Fitting of the decay profiles for both PAHs was achieved using a tri-exponential decay model. Indeed, fitting decay profiles of simple PAHs to a multi-exponential decay in water is not uncommon; in fact two emitting species are often observed, corresponding to the free PAH (shortest lifetime) and a hydrated aggregate cluster species (typically longer-lived);[20] these probes in particular also have the potential for excimer and exciplex formation, emitting species with significantly longer lifetimes.[13a]

For anthracene, contributions were ascribed to two shorter-lived emitting species and one longer-lived one, although the latter had a much smaller contribution to the overall emission (ca. 1%, Table S1). Upon addition of dendrimer, little change was observed in the excited state lifetimes of the two shortest-

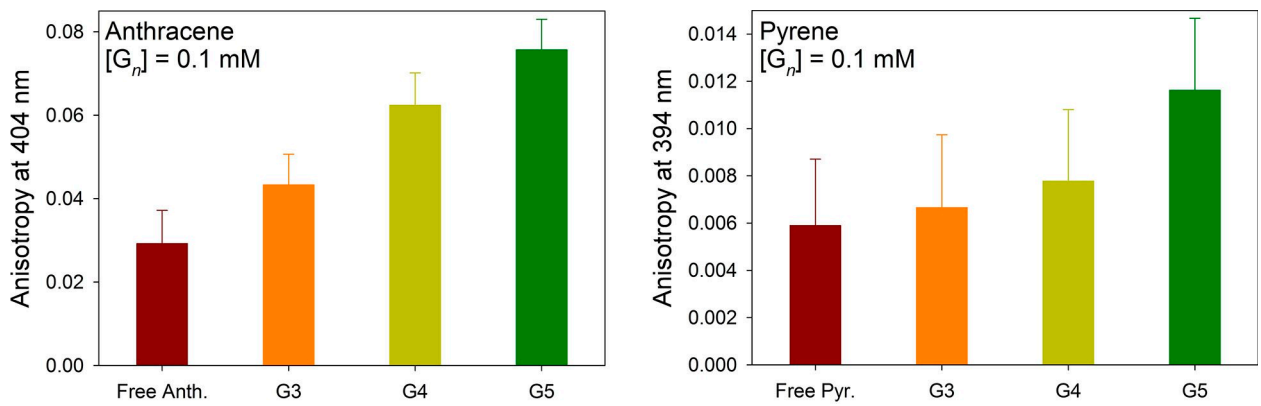

Figure 5. Fluorescence anisotropy data for anthracene (left) and pyrene (right), with constant concentration of G3-G5 PAMAM dendrimer ([G*n*] = 0.1 mM)in water solution containing 7.2% MeOH by volume, buffered to pH 7.4 with 50 mM HEPES (anthracene λ_{exc} = 350 nm; pyrene λ_{exc} = 338 nm).

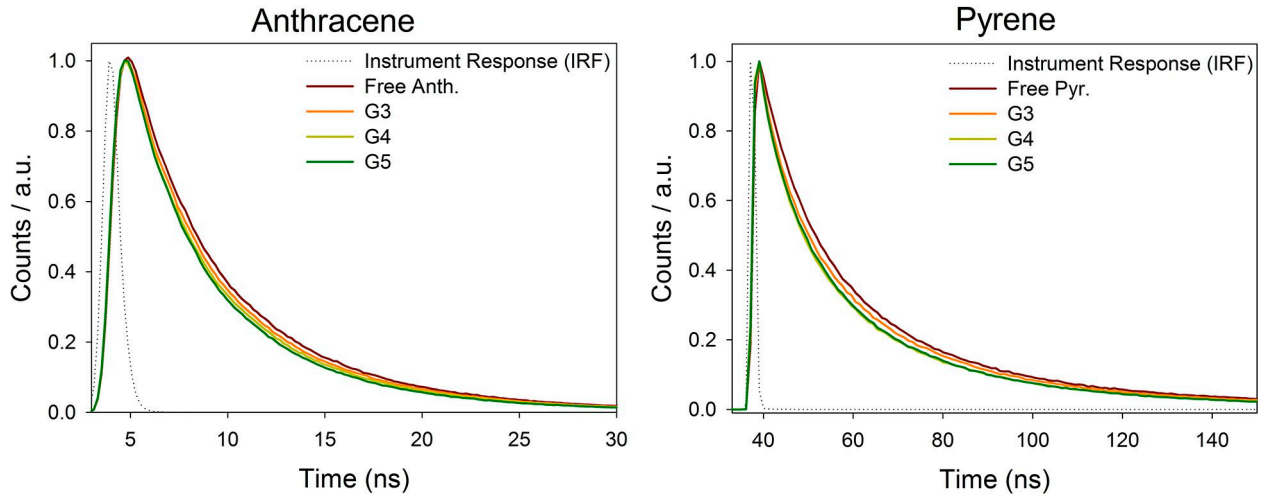

Figure 6. Time-resolved fluorescence decay for anthracene (left) and pyrene (right) in an aqueous solution containing 0.1 mM G3-G5 PAMAM dendrimer and 7.2% MeOH by volume, buffered to pH 7.4 with 50 mM HEPES.

lived contributors to the overall fluorescence emission (i.e. free anthracene in solution and its hydrated aggregate, respectively), suggesting that the dendrimer was incapable of acting as a dynamic (i.e. collisional) quencher on free anthracene in solution. The contribution of the longer-lived emitter increased somewhat in the presence of the dendrimer, but its lifetime was the most significantly reduced of the three.

Contrary to anthracene, pyrene's longest-lived component with an excited state lifetime around 80–100 ns (Table S1), corresponding to the excimer's emission, provided a much greater relative contribution, consistent with our observations in steady-state fluorescence emission experiments. It is interesting to note, however, that in these conditions the longer-lived excimer's contribution is evident even in the absence of the dendrimers. Among the monomeric lifetime components, the shorter-lived species for pyrene displayed a greater decrease in their lifetimes (τ_1 and τ_2) upon interaction with PAMAM than anthracene's, albeit the effect was relatively small for both PAH probes. The more pronounced decrease in pyrene's emitter lifetimes in the presence of these dendrimers suggests that dynamic quenching effects are more prominent for pyrene; this is in line with our previous observations on pyrene's steady-state emission (Figure 4).

In general, the decay profiles for each PAH probe in the presence of [PAMAM] = 0.1 mM, i.e. the same concentration used for the steady-state work described above, were similar across dendrimer generations (Figure 6). This is a particularly important observation in the case of the pyrene probe. In fact, pyrene's emission is quenched in the presence of the dendrimer (Figure 4), which may suggest adventitious interactions between the dendrimer and the PAH, leading to collisional quenching. However, pyrene's excited state lifetime was found to be essentially unaffected by the addition of dendrimer, effectively disproving this possibility and indicating that the observed steady-state quenching was due to the formation of a ground-state complex between the pyrene and the dendrimer (i.e. static quenching).

Fluorescence lifetime measurements were also carried out at a higher concentration of dendrimer (0.84 mM) with both PAH probes, to highlight the different behavior of these two probes when interacting with the same dendritic host. G4 PAMAM was used for this study since it represents the midpoint in generation and size among those we had selected for the current work. Indeed, at higher concentrations of G4 PAMAM dendrimer, we observed a much more significant change in the decay curve of the free vs. bound species for both PAH probes, as shown in Figure 7. The corresponding lifetime parameters obtained from a multi-exponential fit (Table 1) clearly show that there is more substantial decrease in the lifetimes for all emissive species at such high dendrimer

Table 1. Time-resolved fluorescence decay parameters from tri-exponential fitting of the emission decay profiles for anthracene and pyrene in Figure 7 ([G*n*] = 0.84 mM).

	T_1 (ns)	T_2 (ns)	T_3 (ns)	$\%_1$	$\%_2$	$\%_3$
Free Anth.	3.31 ± 0.03	7.33 ± 0.05	24 ± 1	36	63	1
G4 + Anth.	1.86 ± 0.02	5.88 ± 0.04	13.6 ± 0.2	27	65	8
Free Pyr.	10.1 ± 0.2	29.3 ± 0.3	107.7 ± 0.4	18	52	30
G4 + Pyr	3.16 ± 0.05	15.5 ± 0.2	38.8 ± 0.2	19	43	38

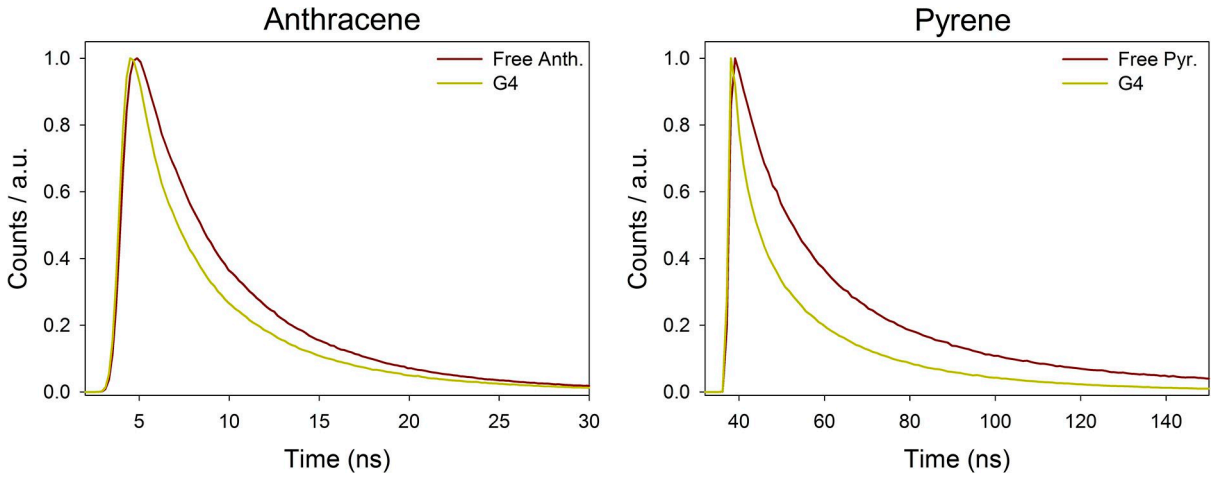

Figure 7. Fluorescence emission decay for anthracene (left) and pyrene (right) with and without G4-PAMAM dendrimer (gold and red lines, respectively, [G4] = 0.84 mM). Each solution contained 15% MeOH by volume in water buffered to pH 7.4 with 50 mM HEPES.

concentrations; expectedly, pyrene displays the greatest change in lifetime compared to anthracene, indicating that pyrene is more susceptible to dynamic quenching with these dendrimers; we hypothesize that this is indicative of its more interior position within the hydrophobic core of these dendrimers upon binding, which leaves it more susceptible to dynamic quenching by the dendrimer's internal tertiary amine groups.

Selective Quenching Experiments. The experimental results discussed so far provide evidence to support distinct interaction modes between each of the two hydrophobic fluorescent probes and the polycationic PAMAM hosts. Based on the steady-state and time-resolved fluorescence measurements shown above, the dendrimer is a more effective quencher for pyrene's fluorescence emission than anthracene's, an effect that we ascribe to the positioning of the pyrene upon binding, deeper inside the PAMAM dendrimer's more hydrophobic core, which leads to more effective quenching of the pyrene's excited state through photoinduced electron transfer from the tertiary amine groups present in the inner core of the dendrimer, a more effective quencher than the terminal primary amines on the macromolecular host's surface.[16b] To independently probe the location of binding of the anthracene and pyrene probes to the dendrimer and support this hypothesis, we conducted cesium(I) selective quenching experiments on complexes of these probes with G3-G5 PAMAM dendrimers.

If binding of the fluorescent aromatic hydrocarbon probes were driven primarily by cation-π interactions, which require the involvement of the protonated primary amines of the dendrimer only found at the surface of the macromolecule, then, even when bound to PAMAM, the participating fluorescent probes would find themselves close to the surface of the polymer and exposed to the bulk solution. Therefore, a hydrophilic cationic quencher such as Cs^+, which would be able to access the solvent-exposed surface of the dendrimer but not its core, due to its hydrophilicity and charge, should effectively quench the fluorescence emission of the fluorescent probe even when bound, regardless of the presence of the dendrimer.

On the other hand, if the PAH probe were encapsulated deeper inside the dendrimer's core upon binding, the Cs^+ cationic quencher would be far less likely to reach the fluorophore, due to electrostatic repulsion between the positively charged ammonium groups and the Cs^+ ions, leading to considerably less effective quenching of the fluorescent probe in the presence of dendrimer vs. in its absence (Scheme 3). Indeed, similar experiments have been conducted to study PAH interactions with various quenching agents in the presence of carboxylate-terminated PAMAM dendrimers.[21]

For these titrations, a saturated solution of each PAH probe in buffered water containing a constant amount of MeOH (7.2% MeOH by volume) was prepared in the same way as the thin film emission experiments described above and added to a clean 1 cm quartz cuvette for titration with Cs^+. Separately, a CsCl titrant solution was prepared in the same solvent system. Aliquots (25–100 μL) of this solution were then added to each cuvette and steady-state fluorescence emission measurements were taken for each PAH probe after each addition. The resultant profiles of emission intensity at the wavelength of maximum emission for the monomer form of each PAH (404 nm for anthracene, 394 nm for pyrene) vs. added Cs^+ are presented in Figure 8. These results clearly show that larger, higher-generation PAMAM dendrimers more effectively protect pyrene's excited state from quenching by the added Cs^+ ions. Anthracene also displayed a similar trend, albeit to a lesser extent. In accordance with our hypothesis, these results indicate that anthracene binds preferentially to the exterior of the dendrimer, likely via cation-π interactions, whereas pyrene is encapsulated within the hydrophobic confines of the dendrimer. This difference is particularly pronounced for the larger G4 and G5 dendrimers. Stern-

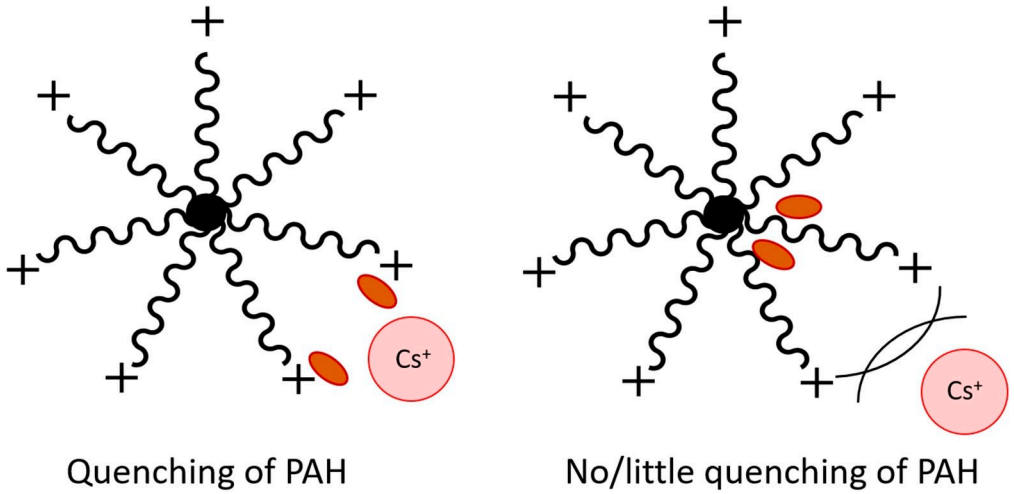

Scheme 3. A schematic representation of the possible interaction modes between Cs^+ with a surface-bound PAH probe (left) vs. an internally encapsulated probe (right). Given the polycationic nature of the poly(amidoamine) dendrimers, PAHs inside the dendrimer would be more effectively shielded from the fluorescence quenching effect of Cs^+ cations.

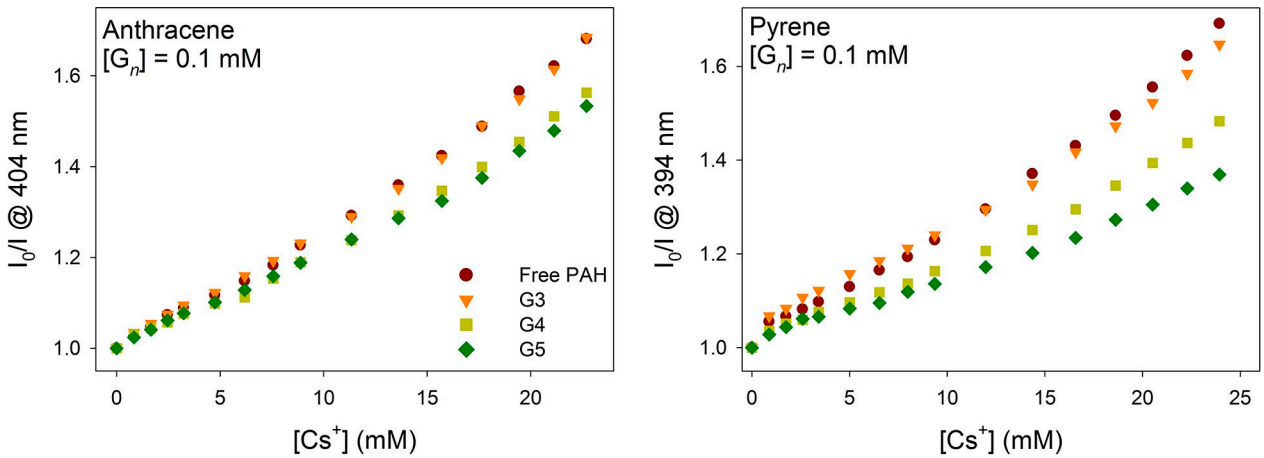

Figure 8. Stern-Volmer plots containing G3-G5 PAMAM dendrimer ([G*n*] = 0.10 mM) for anthracene (left) and pyrene (right), upon the addition of CsCl. All measurements were conducted in a water solution containing 7.2% MeOH by volume, buffered to pH 7.4 with 50 mM HEPES (anthracene λ_{exc} = 350 nm; pyrene λ_{exc} = 338 nm).

Volmer constants (K_{SV}) were estimated for each Cs^+ quenching titration by fitting the first ten points to a linear model (see Supporting Information for details and results). Comparison of the measured K_{SV} values shows that Cs^+ becomes progressively less effective at quenching pyrene as the dendrimer generation increases (i.e. pyrene is more and more effectively shielded from cesium's reach by larger dendrimer generations), once more hinting at its binding in the dendrimer's core, away from the Cs-accessible surface. On the other hand, a much smaller difference in K_{SV} was observed among different generations in the case of anthracene complexes, indicating that anthracene binds much closer to the Cs-accessible surface.

We repeated the Cs^+ quenching experiments at the higher G4 concentration used above, as well ([G4] = 0.84 mM). The CsCl titrant solution was prepared, using an equal H_2O:methanol ratio as the cuvettes (75% H_2O:15% MeOH by volume, buffered to pH 7.4 with 50 mM HEPES). Fluorescence emission spectra were taken after addition of aliquots (25–100 μL) of the CsCl titrant solution. The results from these titrations are presented in Figure 9. Based on these plots, it is apparent that at higher dendrimer concentration pyrene was completely shielded from the quenching effect of the Cs^+ ions, with essentially no change in the steady-state fluorescence emission upon addition of Cs^+ ions. On the other hand, the higher G4-PAMAM concentration did not reduce the quenching of anthracene by Cs^+ ions; in fact, in the case of the anthracene probe we noticed essentially no difference between the lower and higher dendrimer concentration (i.e. [G4 PAMAM] = 0.10 vs. 0.84 mM). Stern-Volmer quenching constants (K_{SV}) were also estimated using the initial linear

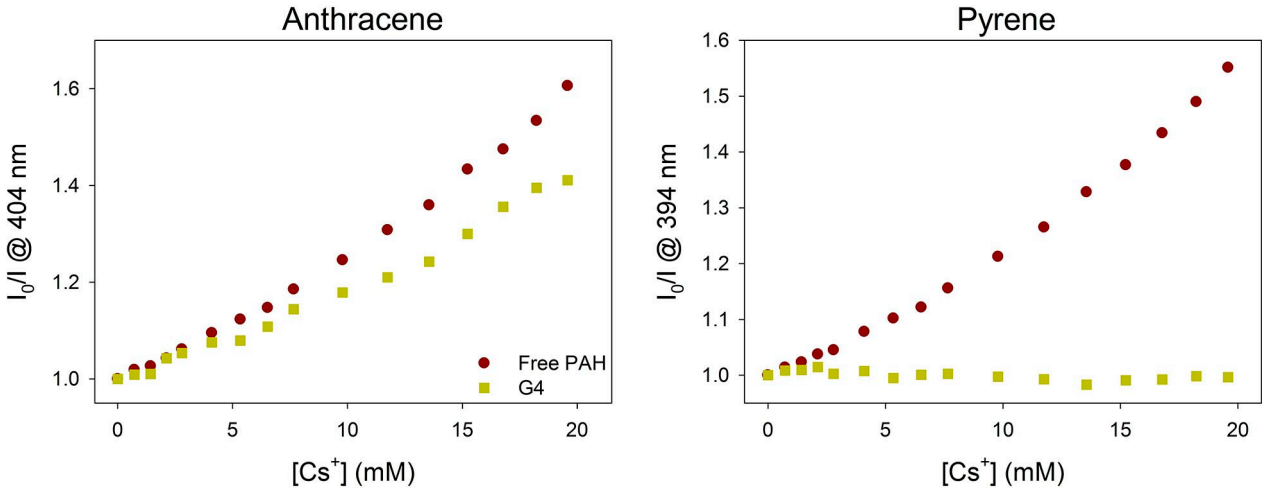

Figure 9. Stern-Volmer plots for the titration of anthracene (left) and pyrene (right) with CsCl with (gold squares) vs. without (red circles) G4 PAMAM dendrimer ([G4] = 0.84 mM). All measurements were conducted in a water solution containing 15% MeOH by volume, buffered to pH 7.4 with 50 mM HEPES (anthracene λ_{exc} = 350 nm; pyrene λ_{exc} = 338 nm).

portion of these curves (see Table S3 in the Supporting Information). The results were once more in accordance with the binding location hypothesis mentioned above.

These results for the two fluorescent hydrocarbon probes, pyrene and anthracene, display interestingly different trends in the binding modes of these probes to amine-terminated PAMAM dendrimers, both as a function of the dendrimer generation and its concentration. The evidence suggests that pyrene is encapsulated deep within the polymer upon binding, whereas anthracene is bound closer to the surface, at the interface with the bulk solution; there it interacts with the protonated termini, presumably through cation-π or CH-π interactions. These binding preferences are interesting and quite distinct, considering the similar chemical structure and properties of these hydrophobic aromatic molecules.

3. Conclusions

Poly(amidoamine) (PAMAM) dendrimers were proven to be capable of binding featureless polycyclic aromatic hydrocarbons (PAHs). By taking advantage of these probes' intrinsic fluorescence emission properties, a series of fluorescence-based experiments were carried out to investigate the extent to which these polymers can be envisioned as supramolecular hosts for such hydrophobic hydrocarbons in water media, particularly expanding on our group's previous finding that these macromolecules exhibit enhanced affinity for guests containing an aromatic moiety over their aliphatic counterparts.[9b] In particular, we were interested in establishing a baseline for their ability to improve the water solubility of this class of compound, and possibly to concentrate them out of solution, with an attention to future applications in sensing and remediation.

Fluorescence anisotropy experiments positively confirmed that spectral changes observed upon interaction of these small-molecule probes with PAMAM dendrimers in water stem from binding of the probes to the dendrimers through a telltale increase in anisotropy signal upon addition of PAMAM, which was also sensitive to the macromolecules' size (generation). Time-resolved fluorescence emission experiments were also conducted, resulting in a greater change in lifetime for pyrene upon interaction with PAMAM, which was ascribed to pyrene's deeper encapsulation within the dendrimer's core upon binding, in closer proximity to tertiary amine groups in the structure, known to be effective dynamic quenchers for simple aromatic fluorophores.

The hypothesis of different binding locations for anthracene vs. pyrene was probed using selective quenching experiments with hydrophilic Cs^+ which, although an effective quencher, can only access the solvent-facing surface of these macromolecules. The results confirmed that anthracene was quenched more effectively by Cs^+, independent of dendrimer generation and concentration, whereas pyrene's emission was significantly less affected by Cs^+ ions for higher dendrimer generation and concentration. This was convincing evidence for the different binding modes *and* binding locations of these PAH probes to PAMAM dendrimers. Our general considerations also indicate that these results should also apply to further members of this family of compounds.

In summary, our results suggest that these dendrimers offer interesting and varied binding modes for poorly water-soluble hydrocarbons in neutral aqueous solution. The different binding modes observed for these two PAHs alone warrant further exploration into similar dendritic interactions with other PAH ring systems and chemical structures. This work opens the door to PAMAM dendrimers' further use as supramolecular hosts for otherwise featureless aromatic guests. These properties bode particularly well for the development of pattern-

based chemical fingerprinting systems for such polycyclic aromatic hydrocarbons, whose toxicological and environmental importance, which varies significantly within their family, make them valuable analytical targets for differentiation and quantitation attempts. Furthermore, the differential binding features of these PAHs, outlined in this paper, can be exploited for many other applications, such as chemical separation and applications in controlled delivery of poorly water-soluble active ingredients.

4. Experimental Section

Materials. Amine-terminated poly(amidoamine) (PAMAM) dendrimers with 1,2-diaminoethane (ethylenediamine, *en*) core were manufactured by Dendritech, Inc. and purchased from Sigma-Aldrich as methanol solutions at different concentrations depending on the dendrimer generation. Dendrimer solutions were stored at 4 °C in a refrigerator. For each dendrimer generation, all experiments were carried out using the same batch (lot number) of dendrimer. Anthracene and pyrene were purchased from Sigma-Aldrich and used as received. 2-[4-(2-hydroxyethyl)piperazin-1-yl]ethanesulfonic acid (HEPES) was purchased from ICI Scientific. All experiments were carried out using a 50 mM HEPES aqueous solution buffered to pH 7.4, prepared by adding an appropriate amount of HEPES free acid to deionized (DI) water; the pH was then adjusted to 7.4 by adding 1.0 M NaOH as needed and monitoring with a combined glass pH electrode, then bringing up to volume. The HEPES concentration was diluted slightly (to between 40–50 mM), depending on the amount of PAMAM dendrimer stock solution (in MeOH) that was added to each cuvette.

Instrumentation. All experiments were conducted at 25 °C, maintained using an external circulating water bath. Steady-state fluorescence measurements were conducted with an ISS PC1 spectrofluorimeter. Excitation was carried out using a broad-spectrum high-pressure xenon lamp (CERMAX, 300 W). Excitation correction was performed through a rhodamine B quantum counter with a dedicated detector. For anthracene, excitation was performed at 350 nm; for pyrene at 338 nm. Emission was recorded over a wavelength range of 370–600 nm for anthracene and 360–600 nm for pyrene. Excitation and emission wavelength selection were carried out by computer-controlled monochromators with manual slits for wavelength resolution control (for anthracene: 8 nm bandwidth for excitation, 4 nm for emission; for pyrene: 8 nm bandwidth for excitation; 2 nm for emission). Detection was through a Hamamatsu red-sensitive PMT. Computer-controlled high-aperture Glan-Thompson calcite polarizers were used in the excitation and emission channels to measure steady-state fluorescence anisotropy.

Fluorescence lifetimes were measured with an Edinburgh Photonics Mini-Tau time-resolved fluorometer using the time-correlated single photon counting technique (TC-SPC). Samples were excited by a picosecond-pulsed LED emitting at 310 nm (EPLED series) with a pulse width of 900 ps. For experiments with anthracene and pyrene, the pulse repetition rate was set to 2 MHz and 0.5 MHz, respectively. Control of the excitation power was achieved through a continuously variable neutral density filter wheel to collect 2–3 % excitation photons per second. A long-pass filter with a 450 nm cut-on wavelength was used for emission selection. Photons were detected by a high-sensitivity photomultiplier tube over a time range of 200 ns (for anthracene) and 1 μs (for pyrene). Decay curves were accumulated for 180 s (3 min.) and the resultant decay data was fit using the multi-exponential iterative reconvolution fit in the Edinburgh T900 software.

Thin film experimental design. Stock solutions of anthracene and pyrene were prepared by adding about 25 mg of solid fluorophore to 25 mL of hexanes. Aliquots (200–300 μL) of fluorophore stock solution were transferred to a 1 cm quartz or untreated polystyrene cuvette and the hexanes was carefully blown off via a nitrogen stream. Care was taken so that the deposition of PAH was below the position of the impinging optical beam of the spectrofluorimeter. Aliquots of water buffered to pH 7.4 with 50 mM HEPES were then added to the cuvette containing the deposited solid PAH, followed by an appropriate aliquot of dendrimer stock solution in methanol. At this point, any deviation from pH 7.4 was corrected by adding a small amount of ~1 M HCl (ca. 3–7.5 μL) before filling to volume (3.0 mL) with more HEPES, to give [PAMAM] = 0.1 mM or 0.84 mM, depending on the experiment. Each cuvette was then sealed tight with Parafilm and stored in the dark at room temperature overnight, letting each solution reach dissolution equilibrium. The cuvettes were then subjected to steady-state fluorescence emission, time-resolved fluorescence lifetime, and fluorescence anisotropy measurements.

For Cs^+ quenching experiments, the supernatant from each equilibrated cuvette was removed and added to a clean 1 cm quartz cuvette. A stock solution of cesium chloride was prepared separately by adding the solid salt to 5 mL HEPES buffer, to give a ca. 0.35 M solution. The Cs^+ titrant solution was made by taking an aliquot of the CsCl stock solution (about 1 mL), adding to HEPES buffer, and then filling to volume with appropriate amounts of buffer and methanol to achieve the same content of MeOH as the cuvette solutions (% by volume). Small aliquots of this Cs^+ titrant solution were added to the cuvette, and a fluorescence emission measurement taken after each addition (excitation at 350 nm for anthracene; at 338 nm for pyrene).

References

[1] a) S. Chandra, S. Dietrich, H. Lang, D. Bahadur, *J. Mater. Chem.* **2011**, *21*, 5729–5737; b) Y. Bae, K. Kataoka, *Adv. Drug Delivery Rev.* **2009**, *61*, 768–784.
[2] E. Buhleier, W. Wehner, F. Voegtle, *Synthesis* **1978**, 155–158.
[3] C. J. Hawker, K. L. Wooley, J. M. J. Frechet, *J. Chem. Soc. Perkin Trans. 1* **1993**, 1287–1297.

[4] D. A. Tomalia, H. Baker, J. Dewald, M. Hall, G. Kallos, S. Martin, J. Roeck, J. Ryder, P. Smith, *Polym. J.* **1985**, *17*, 117–132.
[5] a) Y. Niu, L. Sun, R. M. Crooks, *Macromolecules* **2003**, *36*, 5725–5731; b) D. Cakara, J. Kleimann, M. Borkovec, *Macromolecules* **2003**, *36*, 4201–4207.
[6] a) I. J. Suarez, R. Rosal, A. Rodriguez, A. Ucles, A. R. Fernandez-Alba, M. D. Hernando, E. Garcia-Calvo, *TrAC Trends Anal. Chem.* **2011**, *30*, 492–506; b) P. E. S. Smith, J. R. Brender, U. H. N. Durr, J. Xu, D. G. Mullen, M. M. Banaszak Holl, A. Ramamoorthy, *J. Am. Chem. Soc.* **2010**, *132*, 8087–8097; c) B. Klajnert, A. Pastucha, D. Shcharbin, M. Bryszewska, *J. Appl. Polym. Sci.* **2007**, *103*, 2036–2040.
[7] a) A. M. Mallet, Y. Liu, M. Bonizzoni, *Chem. Commun.* **2014**, *50*, 5003–5006; b) Y. Liu, M. Bonizzoni, *J. Am. Chem. Soc.* **2014**, *136*, 14223–14229.
[8] X. Liang, M. Bonizzoni, *J. Mater. Chem. B* **2016**, *4*, 3094–3103.
[9] a) A. M. Jolly, M. Bonizzoni, *Supramol. Chem.* **2015**, *27*, 151–160; b) A. M. Jolly, M. Bonizzoni, *Macromolecules* **2014**, *47*, 6281–6288; c) M. Bonizzoni, S. R. Long, C. Rainwater, E. V. Anslyn, *J. Org. Chem.* **2012**, *77*, 1258.
[10] a) D. Yan, S. Wu, S. Zhou, G. Tong, F. Li, Y. Wang, B. Li, *Environ. Pollut.* **2019**, *248*, 804–814; b) W. Du, X. Li, Y. Chen, G. Shen, *Environ. Pollut.* **2018**, *237*, 625–638; c) B. K. Behera, A. Das, D. J. Sarkar, P. Weerathunge, P. K. Parida, B. K. Das, P. Thavamani, R. Ramanathan, V. Bansal, *Environ. Pollut.* **2018**, *241*, 212–233; d) G. Adamkiewicz, H. Choi, J. M. Delgado Saborit, P. Fharrison, R. M. Harrison, R. F. Henderson, D. Jarvis, D. A. Kaden, F. J. Kelly, S. Kephalopoulos, H. Komulainen, D. Kotzias, M. Kreuzer, C. Mandin, R. L. Maynar, J. McLaughlin, G. Nielsen, N. Nijhuis, D. G. Penney, N. Shinohara, P. Wolkoff, M. Krzyzanowski, *WHO guidelines for indoor air quality: selected pollutants*, World Health Organization Regional Office for Europe, Copenhagen, **2010**; e) C. A. Menzie, B. B. Potocki, J. Santodonato, *Environ. Sci. Technol.* **1992**, *26*, 1278–1284.
[11] a) K.-H. Kim, S. A. Jahan, E. Kabir, R. J. C. Brown, *Environ. Int.* **2013**, *60*, 71–80; b) A. M. Mastral, M. S. Callen, *Environ. Sci. Technol.* **2000**, *34*, 3051–3057.
[12] J. Tropp, M. H. Ihde, A. K. Williams, N. J. White, N. Eedugurala, N. C. Bell, J. D. Azoulay, M. Bonizzoni, *Chem. Sci.* **2019**, *10*, 10247–10255.
[13] a) J. R. Lakowicz, *Principles of Fluorescence Spectroscopy*, Springer, New York, NY, **2013**; b) J. Duhamel, *Langmuir* **2012**, *28*, 6527–6538.
[14] K. Gowthamarajan, S. K. Singh, *Dissolution Technol.* **2010**, *17*, 24–33.
[15] L. Fernandez, M. Gonzalez, H. Cerecetto, M. Santo, J. J. Silber, *Supramol. Chem.* **2006**, *18*, 633–643.
[16] a) I. Arias-Gonzalez, J. Reza, A. Trejo, *J. Chem. Thermodyn.* **2010**, *42*, 1386–1392; b) J. V. Goodpaster, V. L. McGuffin, *Anal. Chem.* **2000**, *72*, 1072–1077.
[17] Y. Niu, L. Sun, R. M. Crooks, *Macromolecules* **2003**, *36*, 5725.
[18] a) M. J. Jasmine, M. Kavitha, E. Prasad, *J. Lumin.* **2009**, *129*, 506–513; b) D. Wang, T. Imae, M. Miki, *J. Colloid Interface Sci.* **2007**, *306*, 222–227; c) D. Wang, T. Imae, *J. Am. Chem. Soc.* **2004**, *126*, 13204.
[19] a) B. Bardi, M. Krzeszewski, D. T. Gryko, A. Painelli, F. Terenziani, *Chem. Eur. J.* **2019**, *25*, 13930–13938; b) Y.-C. Chen, Z. Wang, M. Yan, S. A. Prahl, *Luminescence* **2006**, *21*, 7–14; c) J. Marczyk, J. C. Fetzer, J. Szubiakowski, J. Waluk, *J. Lumin.* **1997**, *72–74*, 517–519.
[20] a) K. M. Chan, W. Xu, H. Kwon, A. M. Kietrys, E. T. Kool, *J. Am. Chem. Soc.* **2017**, *139*, 13147–13155; b) A. Ganguly, S. Ghosh, N. Guchhait, *Photochem. Photobiol. Sci.* **2015**, *14*, 2168–2178; c) R. Alonso, M. Yamaji, M. C. Jimenez, M. A. Miranda, *J. Phys. Chem. B* **2010**, *114*, 11363–11369; d) Y. Shiraishi, Y. Tokitoh, T. Hirai, *Org. Lett.* **2006**, *8*, 3841–3844.
[21] a) D. A. Wade, C. Mao, A. C. Hollenbeck, S. A. Tucker, *Fresenius J. Anal. Chem.* **2001**, *369*, 378–384; b) D. A. Wade, P. A. Torres, S. A. Tucker, *Anal. Chim. Acta* **1999**, *397*, 17–31.

Manuscript received: November 10, 2020
Revised manuscript received: December 23, 2020
Version of record online: February 19, 2021